

Effect of the Aligned Flow Obstacles on Downward-Facing CHF in an Inclined Rectangular Channel

Uiju Jeong, Hong Hyun Son, Gwang Hyeok Seo, Gyoodong Jeun, Sung Joong Kim*
Department of Nuclear Engineering, Hanyang University,
222 Wangsimni-ro, Seongdong-gu, Seoul, 133-791, Republic of Korea

1. Introduction

Recently, a design concept of ex-vessel corium cooling system using an external core catcher has been proposed as one of severe accident mitigation measures for an APR1400 [1]. Under the severe accident where corium fail the reactor vessel, the water of the In-containment Refueling Storage Tank (IRWST) feeds into the cooling channel underneath the core catcher so that a natural circulation occurs. The detailed information for the engineered corium cooling system is schematically presented in Fig. 1. In the core catcher system, a key design component of our interest is the engineered corium cooling system, consisting of an engineered cooling channel made of a single channel between the corium spreading compartment and inside wall of the cavity, and many short columnar structures, called stud, supporting the loading on the core catcher body. The cooling channel consists of the inclined (10°) portion of the downward facing heating channel and vertical portion of the heating channel. Features unique to flow boiling with the downward-facing heater surface in the inclined cooling channel where the studs are installed have drawn a considerable attention. That's because prior studies on boiling crisis indicate the orientation of the heated wall can exert substantial influence on CHF [2,3]. Especially, the concentration of the vapor near the downward facing heater surface makes this region susceptible to premature boiling crisis when compared to vertical or upward-facing heated wall. Also, the installed studs could cause a partial flow blockage, and distort the flow streamline. Due to the distortion, stagnation points may occur in the cooling channel, promoting the concentration of the vapor near the heated wall. Then, the locally degraded heat transfer around the points may result in the formation of vapor pocket.

The primary objective of this study is to make available experimental data on the CHF values varying the shape of studs and to improve understanding of the mechanism of flow boiling crisis associated with the aligned flow obstructions by means of visual experimental study. This study presents experimental data for subcooled flow boiling of water at atmospheric pressure and low mass flux conditions.

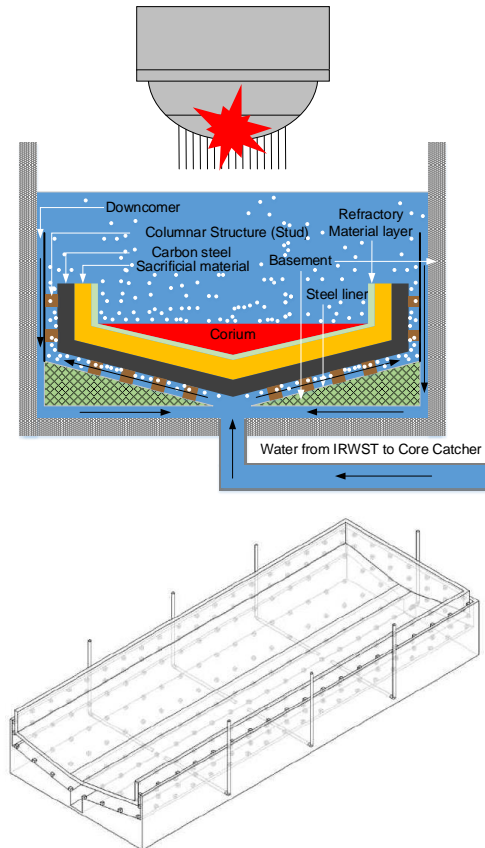


Fig. 1. Schematics of the engineered corium cooling system.

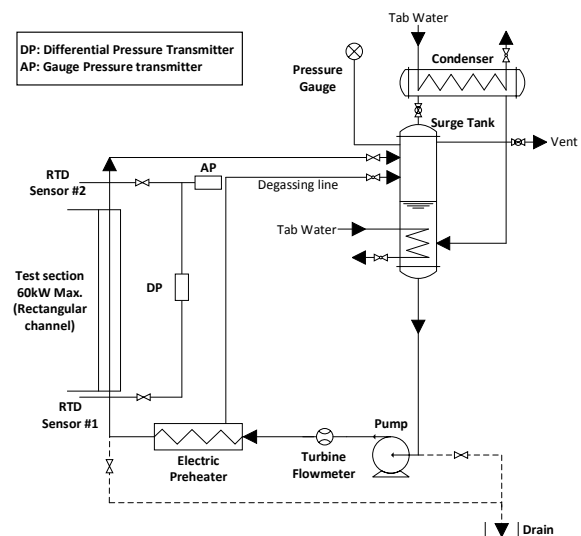


Fig. 2. Schematic of the forced convection boiling loop.

2. Experimental Setup

The visual study using the high speed camera in subcooled flow boiling of water has been performed using the water boiling loop, schematically shown in Fig. 2. It has been built recently and since then operated for the purpose of investigating subcooled flow boiling process with downward facing heat transfer for the inclined engineered cooling channel.

This loop is a low-pressure system with the piping made of SUS316. Circulation of water through the loop is made and controlled by a centrifugal pump with a variable-frequency drive. The fluid bulk temperatures are measured by 4-wire RTD sensors and controlled by the pre-heater located upstream of the test section. Electrical signal from the K-type (chromel/alumel) thermocouples, RTD sensors, flow meter, pressure transducers, voltage/current/power meter are collected through the National Instrument SCXI-cDAQ series devices. The digitized data are collected by NI LabVIEW software and stored on the computer. The measurements of the signals were carried out with time interval of 0.2 s.

A high-speed video camera (Phantom V7.3) was used to capture the boiling phenomena at a photographing rate of 2000 frames/s.

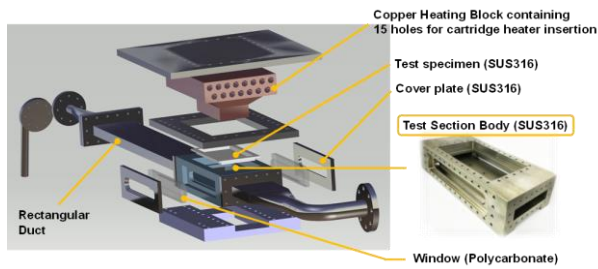


Fig. 3. 3D schematic of the test section.

A 3D schematic of the test section in the boiling loop is presented in Fig. 3, while a cross sectional view of the test section is presented in Fig. 4. The test section mainly consists of a copper block, test specimen and test section body made of SUS316, rectangular ducts. The test section is supported on an adjustable lifting table to replace the test specimen. The major part of the test section is a test section body which is a rectangular channel with dimensions of 30mm (height) x 131.5mm (width) x 400mm (length), inclined by 10° from the horizontal plane. As shown in Fig. 3, there is a copper block containing 15 holes where 4kW capacity cartridge heaters are inserted to serve as the heating element. Heat generated from the heaters is applied to the test specimen, which is in direct contact with water in the channel, through the copper block. The test specimen acts as upper wall of the rectangular channel. The active heat transfer area at the test specimen is considered to

be equal to the contact area between the specimen and copper block, 95.5mm (width) x 203mm (length).

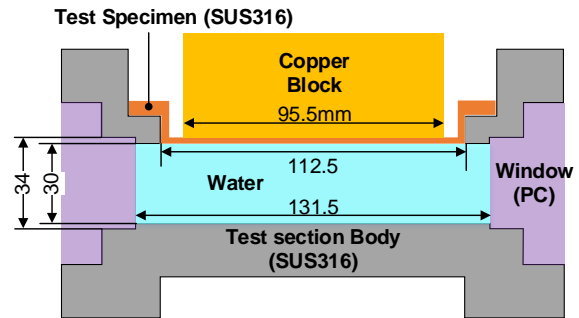


Fig. 4. Cross sectional view of the test section.

To calculate heat flux applied to the test specimen, three K-type, each spaced 8 mm apart, were used to measure the temperature gradient near the contact surface between the test specimen and copper block. The heat flux and the temperature gradient were calculated using a three point backward space Taylor Series approximation as follows:

$$q'' = -k_{cu} \frac{dT}{dx} \quad (1)$$

$$\frac{dT}{dx} = \frac{3T_w - 4T_m + T_d}{2\Delta x} \quad (2)$$

where, T_w , T_m and T_d are copper block temperatures in order of distance from the heat transfer surface.

In order to estimate the distribution of heat flux and wall temperature on the heat transfer surface, 5 sets of thermocouples and 8 thermocouples were positioned at the specific locations, as presented in Fig. 5.

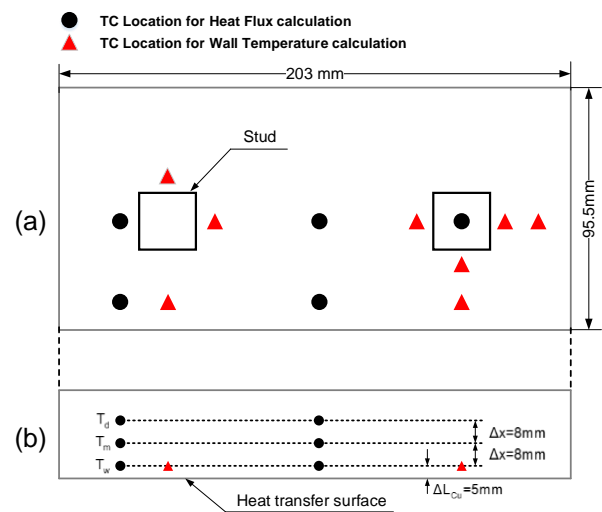


Fig. 5. Distribution of the thermocouples installed in the copper block; (a) Bottom view, (b) Side view.

3. Experimental Procedure

The loop was first filled completely with tap water and then circulated with the pre-heater power on for degassing process for several hours. Boiling experiment proceeded by controlling the a-c power input to the inserted cartridge heaters through Silicon Controlled Rectifier (SCR). In order to obtain reliable experimental data, the electrical power is delivered to the test section with the power step of 0.3 kW once the calculated heat flux is sufficiently in steady state condition. The visualization of the boiling phenomena was performed using a high-speed camera under the arrangement shown in Fig. 6. Capturing the phenomena in the test section is complicated by several factors, such as large scale of heat transfer area unlike very small scale of bubbles, difficulty in defining the exact position where CHF occurs, limited recordable space domain associated with the required large image magnification process.

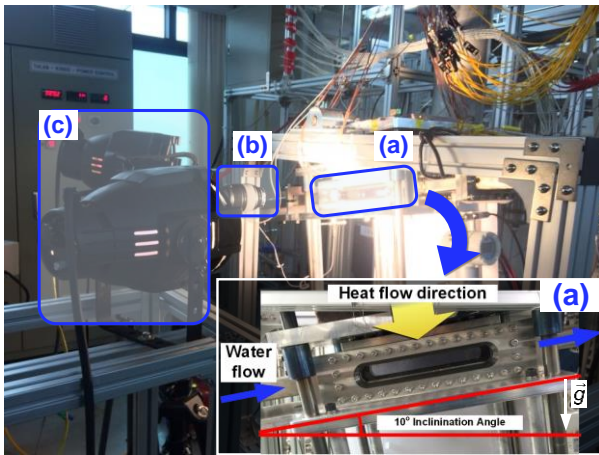


Fig. 6. Arrangement of high-speed camera system; (a) test section, (b) high-speed camera, (c) light source.

4. Results and Discussion

The above experimental procedure was carried out for a test section outlet pressure of 108 kPa, mass flux of $\sim 220 \text{ kg/m}^2\text{-sec}$ and inlet bulk fluid temperature of $\sim 96.5 \text{ }^\circ\text{C}$ ($\Delta T_{\text{sub}}=5\text{K}$). The mass flux condition was determined based on the numerical analysis on the core catcher cooling system using a 1D code MARS. Test specimens made of SUS316 were carefully polished using silicon carbide sandpaper of grit 800.

4.1 CHF without stud structures

The experimental results of the critical heat flux in the test section where studs are not installed were first obtained. These results were compared with the previous data for the downward facing heat transfer in rectangular channel, as plotted in Fig. 7 [2,4,5].

$$q_{cr}(\theta) = \frac{\pi}{24} \rho_v h_{fg} \sqrt{\frac{g \sigma (\rho_l - \rho_v)}{\rho_v^2}} |\sin(180 - \theta)|^{1/2} \times \left(1 + 0.102 \left(\frac{\rho_v}{\rho_l} \right)^{1/4} \frac{c_{pl} (T_{sat} - T_l)}{h_{fg}} \right) \quad (3)$$

$$q_{cr}(\theta) = 276 + 12.6\theta \text{ kW m}^{-2} \quad 5^\circ < \theta < 30^\circ \quad (4)$$

$$q_{cr}(\theta) = \sqrt{\rho_g h_{fg}} \left[0.034 + 0.0037\theta^{0.656} \right] \times \left[\sigma (\rho_f - \rho_g) g \right]^{0.25} \quad (5)$$

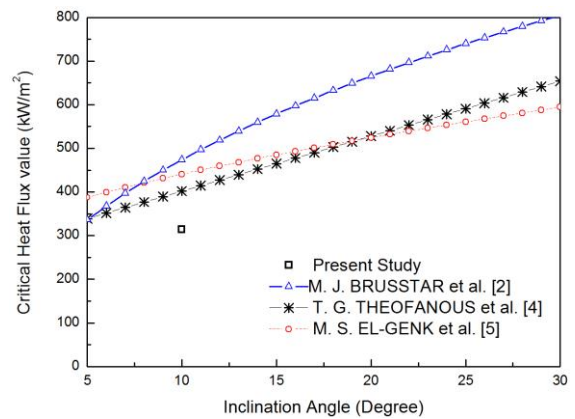


Fig. 7. Measured CHF as a function of inclination angle, compared with the existing CHF correlations.

As presented in Fig. 7, the CHF value from present study is significantly lower than the values from the existing correlations even considering the uncertainty in the experiments. Furthermore, the existing correlations were obtained from the pool boiling experiments where the buoyancy force is dominant while present results were obtained from the subcooled flow boiling experiments. This discrepancy may be emerged from difference in the surface finish of heating wall which is in direct contact with fluid. As is well known, the surface finish may significantly affect nucleation boiling, and therefore the CHF. It means that the aging of heating surface could affect the CHF. According to previous study, it is reported that aging effect, especially oxidation, on the heater surface affect positively on the CHF enhancement [6]. In the previous studies [4-6], material of the heating wall is a pure copper which apt to be oxidized under boiling process, whereas heating wall in this study is made of SUS 316 which has good resistance to oxidation. In consideration of aging effects on the CHF enhancement, it is regarded that the present results on bare CHF sufficiently agree with the previous data. This means that proper operation of the boiling loop is verified, together with the accuracy of the data acquisition system.

4.2 CHF with stud structures

To investigate the heat transfer capability of the lab-scale core catcher cooling channel, four studs were installed in the inclined rectangular channel in a line. The arrangement of the studs is described in Fig. 5. In this study, the shape of the stud is limited to a square column and dimensions of the stud are 25 x 25 x 30 mm³ in length, width and height, respectively. Two of the four studs were in direct contact with the heat transfer area, and the other two were installed at the entrance and exit in the channel each to eliminate the entrance and exit effect.

The measured CHF value is plotted and compared with the CHF data from previously performed bare test, as shown in Fig. 8. The CHF value is remarkably decreased as columnar structures are installed in the channel. By examining the change in heat flux distribution with time, it is confirmed that formation and extinction of local dryout occurs repeatedly just behind the first stud at heat flux of ~160 kW/m². As one of causes of the remarkable decrease in CHF, a slight gap between the upper surface of the stud and the heat transfer surface is considered at present. There is a potential for early dryout initiated from overheating at the slight gap where dryout is expected to occur at low heat flux [3].

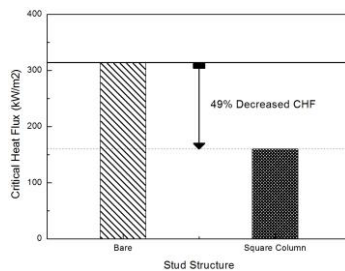


Fig. 8. CHF data of bare and stud equipped.

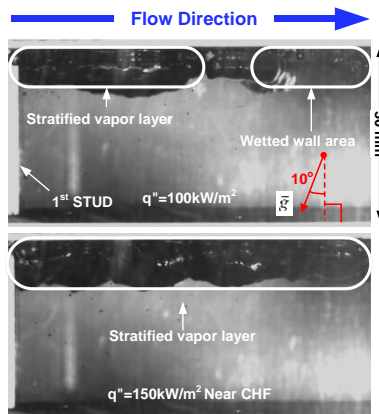


Fig. 9. Boiling images as a function of heat flux.

Fig. 9 shows the high speed images captured at a frame rate of 2000 fps for the channel where studs were

installed. The images show the nucleate boiling regime in the moderate and high heat flux condition.

5. Conclusions

For this study, flow boiling experiments were conducted to estimate the influence of columnar structure in the rectangular channel on downward facing critical heat flux. The major outcomes from this investigation can be summarized as follows:

- (1) The CHF value from bare test section is ~320kW/m², significantly lower than the values from the existing correlations even considering the uncertainty in the experiments.
- (2) The CHF value is remarkably decreased as columnar structures are installed in the channel. It is confirmed that formation and extinction of local dryout occurs repeatedly just behind the first stud at heat flux of ~160 kW/m².
- (3) There is a potential for early dryout initiated from overheating at the slight gap where dryout is expected to occur at low heat flux.

Acknowledgement

This research was supported by the National R&D Program through the National Research Foundation of Korea (NRF) funded by the Korean Government (MSIP) (No. 2014M2B2A9032081) and the Nuclear Safety Research Program through the Korea Foundation of Nuclear Safety (KOFONS), granted financial resource from the Nuclear Safety and Security Commission (NSSC), Republic of Korea (No. 1403002).

REFERENCES

- [1] K. S. Ha, F. B. Cheung, J. Song, R. J. Park and S. B. Kim, Prediction of boiling-induced natural-circulation flow in engineered cooling channels, Nuclear Technology, Vol. 181(1), p.196, 2013.
- [2] M. J. Brusstar, H. Merte, R. B. Keller and B. J. Kirby, Effects of heater surface orientation on the critical heat flux—I. An experimental evaluation of models for subcooled pool boiling, International journal of heat and mass transfer, Vol.40(17), p.4007, 1997.
- [3] Y. H. Kim and K. Y. Suh, One-dimensional critical heat flux concerning surface orientation and gap size effects, Nuclear engineering and design, Vol.226(3), p.277, 2003.
- [4] M. S. El-Genk and Z. Guo, Transient boiling from inclined and downward-facing surfaces in a saturated pool. International journal of refrigeration, Vol.16(6), p.414, 1993.
- [5] T. G. Theofanous, S. Syri, T. Salmassi, O. Kymäläinen and H. Tuomisto, Critical heat flux through curved, downward facing, thick walls. Nuclear Engineering and Design, Vol.151(1), p.247, 1994.
- [6] H. H. Son, U. Jeong, G. H. Seo, G. Jeun and S. J. Kim, effect of wettability and capillary wicking changes induced by oxidation on the pool boiling critical heat flux, Proceedings of The International congress on Advances in Nuclear Power Plants (ICAPP-2015), May.3-6, 2015, Nice, France.